Comparison of the Reactivity between Linear and Cyclic Spin Traps containing Diphenylphosphinoyl moiety

Kosei SHIOJI*, Hidefumi IWASHITA, Noriyoshi NAGAHORA and Kentaro OKUMA

（Received November 30, 2016）

Abstract

Cyclic and acyclic spin traps containing diphenylphosphinoyl moiety were prepared by the microwave addition followed by the oxidation with OXONE. The spin traps were used in ESR spin trapping experiments of carbon, oxygen, and sulfur centered radicals in order to understand their effects. In this experiments, corresponding signals for the radical adducts of the spin traps were observed. Spin trapping of bulky sulfur centered radicals, such as a glutathiyl radical, was found to be influenced by steric hindrance around the C=N bond of spin traps.

Introduction

The conductance of reactive oxygen species (ROS) and their related free radicals have been widely studied because these species cause oxidative stress to cardinal cellular component, such as lipid, protein, and nucleic acid [1]. Detection of these reactive species by ESR measurement using spin traps was influential methodology to understand an oxidative stress that causes a breakdown in the balance between pro-oxidative and anti-oxidant in organisms. The nitrone, 5,5-Dimethyl-1-pyrroline-*N*-oxide (DMPO), was very popular as a spin trap [2-5], however, it has some disadvantages. For example, the adduct of superoxide anion radical ($O_2^{\bullet-}$) has short life time and disproportionation occurred to give an ESR signal of hydroxyl radical adduct. Recently, it has been reported that dihydropyrroline *N*-oxides, substituted by electron withdrawing group at 5-position, trapped superoxide anion radicals to give stable adducts [6-8]. Nolth et al. have reported that the spin trap, diethoxyphosphoryl substituted pyrroline *N*-oxide, 5-(diethoxyphosphoryl)-5-methyl-1-pyrroline *N*-oxide (DEPMPO) gave oxygen radical adducts indicating the higher persistency [9]. They also reported that no spontaneous decomposition was observed and the trapped radical structure was easily identified by phosphorus coupling [9]. The phosphoryl substitution was found to be effective for the stability of radical adducts of linear type spin traps [10, 11]. In our previous study, we have reported that the novel spin traps containing diphenylphosphoryl moiety at 5 position of pyrroline ring, 5-(diphenylphosphinyl)-5-methyl-1-pyrroline *N*-oxide (DPhPMPO) [12-14], and linear nitrone, propylidene-1-diphenylphosphoryl-1-methylethylamine *N*-oxide (PDPhPN) [15], had high affinity toward hydroxyl radicals ($HO^{\bullet}$) and superoxide anion radicals. The corresponding adducts had sufficient life time for ESR measurement. Higher membrane permeability of DPhPMPO was clearly shown by competitive spin trapping through the human erythrocyte ghost [16]. Thus, DPhPMPO can be expected to be useful for *in vivo* ESR measurement. It has been known that oxidative stresses *in vivo* caused by ROS produce some related oxygen, carbon, and sulfur-centered radicals. For example, lipid peroxidation can give several kinds of lipid-derived O and C-centered radicals, such as alkoxy ($RO^{\bullet}$), peroxy ($ROO^{\bullet}$), and alkyl ($R^{\bullet}$) radicals, in addition to hydrophilic $O_2^{\bullet-}$ and $HO^{\bullet}$ [17-19]. Due to the complexity of biological systems, it is difficult to assign radical species. Glutathione is considered to be a major intracellar primary antioxidant, which forms thiyl radical during their activity [20]. ESR-spin trapping is one of the physical techniques that can unambiguously detect glutatiyl radical ($GS^{\bullet}$) in biological system. A downside of DMPO is that although it can trap this radical to form a radical adduct, the spectral parameters are similar to that of hydroxyl radical ($HO^{\bullet}$) adduct [21-23]. Furthermore, hyper fine coupling constants (a_x) determined from ESR-spin trapping provide information on a central atom of additional radical species. Since ROS *in vivo* generate

* Department of Chemistry, Faculty of Science, Fukuoka University, Jonan-Ku, Fukuoka 814-0180
e-mail: shioji@fukuoka-u.ac.jp

various radicals having the same central atom with different substituent, the information about the size of radicals is required for monitoring the radical reaction. Here, we have reported the detection and characterization of C-, O-, and S-centered radical adducts of DPhPMPO, PDPhPN and EDPhPN. The report herein also describes that the alkyl chain length and flexibility around the imino bond of spin traps were predominant for the reactivity of these spin traps toward bulky radical such as gultathiyl radical.

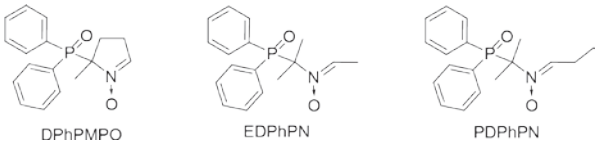

Results and Discussion

Syntheses of DPhPMPO, EDPhPN and PDPhPN. Synthesis of DPhPMPO was described in our previous report [13]. PDPhPN was synthesized from diphenylphosphine oxide and isopropylidene ethylamines using microwave irradiation followed by oxidation with OXONE [15]. EDPhPN was also synthesized from isopropylidene methylamines in the similar manner with 27% total yield. The structures were confirmed by ^{1}H, ^{13}C, ^{31}P NMR, ESI-MS, elemental analysis, and X-ray crystallographic analysis. The ORTEP drawings were shown in Figure 1.

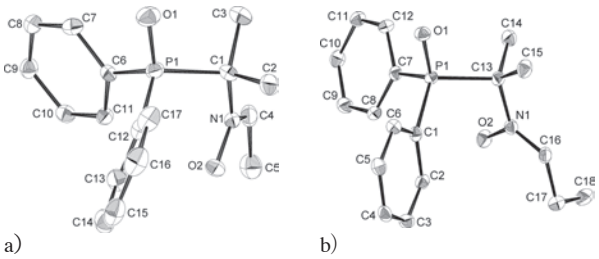

Figure 1 ORTEP Drawings of a) EDPhPN and b) PDPhPN

The microwave reactions were completed within minutes with the favorable yields. These methods were also applied to the synthesis of DPhPMPO. The preparation of precursor amine of DPhPMPO in CH_2Cl_2 under microwave irradiation was completed in a minute with 40% yield (Scheme 1). Partition coefficients of DPhPMPO and PDPhPN were described in the literature [15, 16] and the coefficient of EDPhPN (K_p = 2.2) was determined similarly. The coefficients indicate that EDPhPN and PDPhPN spin traps were more lipophilic than DEPMPO and DMPO. The crystal structures of EDPhPN and PDPhPN suggest that C=N double bond was covered with diphenylphosphinoyl moiety. ^{1}H NMR chemical shifts for olefinic proton of DPhPMPO, EDPhPN, and PDPhPN were 6.66, 6.88, and 6.69 ppm, respectively. Due to the shielding effect by benzene ring, these values were shifted to higher field compared to that of DEPMPO (7.00 ppm). The results also indicate that diphenylphosphinoyl moiety was close to C=N double bond in solution.

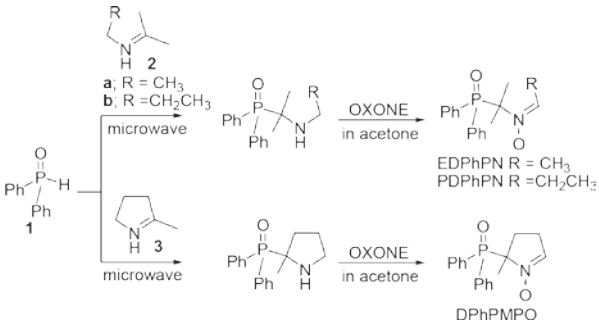

Scheme 1 Synthesis of DPhPMPO using microwave irradiation.

ESR Studies. (a) Spin Trapping of Hydroxyl Radicals and Superoxide Anion Radical. Hydroxyl radical was generated by Fenton system (H_2O_2-$FeCl_2$) in phosphate buffer in the presence of each spin trap DPhPMPO, EDPhPN and PDPhPN, and the ESR signals of corresponding adducts were detected. DPhPMPO/$HO^{\bullet}$ signal composed a double quartet which was attributed to similar hyperfine splitting constants of N and H, and the large phosphorus coupling further split the quartet. On the other hand, the signal of PDPhPN/$HO^{\bullet}$ showed six doublets which were attributed to triplets with a small hyperfine coupling of hydrogen (a_H) and large phosphorus coupling. Superoxide anion radical was trapped at pH 7.2 using DPhPMPO, EDPhPN or PDPhPN in superoxide-generating systems. Typically, ESR signals were detected when superoxide was generated in the presence of DPhPMPO. However, five broad lines was observed when superoxide was trapped by PDPhPN. Since the ESR spectra of PBN/$HO^{\bullet}$ and PBN/$O_2^{\bullet-}$ with very close hyperfine splitting constants are similar, it can be a misinterpretation in spin trapping experiment. In this study, we found that the difference between the ESR spectra of PDPhPN/$HO^{\bullet}$ and PDPhPN/$O_2^{\bullet-}$ was obvious, for example, $HO^{\bullet}$ and $O_2^{\bullet-}$ trappings of EDPhPN proceeded to give corresponding signals. The broadening of the signal was observed when $O_2^{\bullet-}$ was trapped by EDPhPN. In pyridine, $O_2^{\bullet-}$ trappings with these spin traps were also successful to give corresponding ESR signals. These signals and

their computer simulation were described in Figure 2. Hyperfine splitting constants of these radical adducts were summarized in Table 1.

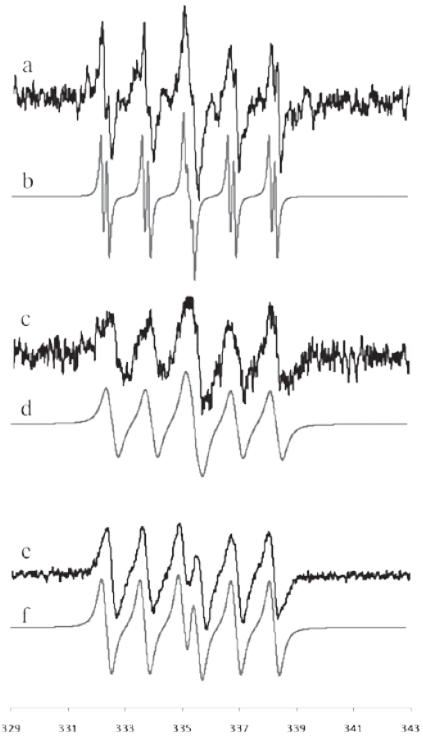

Figure 2 ESR signals of $HO^{\bullet}$ and $O_2^{\bullet-}$ adduct of EDPHPN and their computer simulation. (a) shows EDPHPN/$HO^{\bullet}$, (b) shows computer simulation of (a), (c) shows EDPHPN/$O_2^{\bullet-}$, (d) shows computer simulation of (c), (e) shows EDPHPN/$O_2^{\bullet-}$ in pyridine, and (f) shows computer simulation of (e).

(c) Spin Trapping of Other Radicals with DPhPMPO.

The spin trappings of the methyl radical, *tert*-butoxy radical, *tert*-butoxyperoxyl radical, and thiyl radical generated by appropriate conditions with DPhPMPO were performed in the deoxygenated DMSO (Scheme 2). The ESR spectra of the DPhPMPO/$R^{\bullet}$ have been simulated as a combination of conformers. Computer simulation of experimental spectra was used for the calculation of hyper fine coupling constants (hfsc's) and was summarized in Table 2. The composite simulation showed two ESR spectra with the ratio of approximately 85:15 component except for the methyl thiyl radical adduct.

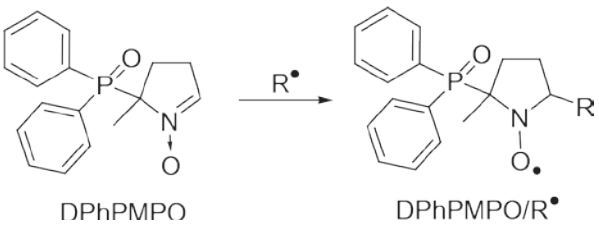

Scheme 2 Spin Trapping of Several radicals with DPhPMPO.

Each a_H and a_N values were similar to those of counterpart. Only a_P values were different in each conformer's. These phenomena were resembled to the results of trapping experiment using DEPMPO derivatives [24]. To investigate the ability of DPhPMPO in trapping free radicals arising from lipid peroxidation processes, spin-trapping experiments were conducted with linoleic acid hydroperoxide, used as a model of peroxidized polyunsaturated fatty acids. Linoleic acid hydroperoxide generated from air-oxidation [25] of linoleic acid was reacted with DPhPMPO to give a signal of the adduct (a_N = 1.32 mT, $a_{H\beta}$= 1.16 mT, a_P = 4.03mT). Figure 3 shows the composite ESR spectrum between DPhPMPO/$LO^{\bullet}$ and DPhPMPO/$HO^{\bullet}$ obtained in an aerobic incubation of linoleic hydroperoxide and Fe^{2+} in phosphate buffer containing DPhPMPO. The similar result was previously reported by Stolze et al. [26, 27] and aided our analysis.

TABLE 1 ESR Hyperfine Splitting Constants for Hydroxyl and Superoxide Radical Adducts of DPhPMPO, EDPhPN, and PDPhPN

adduct	source	solvent	a_N (mT)	a_H (mT)	a_P (mT)	ref
DPhPMPO/$HO^{\bullet}$	H_2O_2-Fe^{2+}	PBS	1.38	1.39	3.56	12
DPhPMPO/$O_2^{\bullet-}$	HX-XO	PBS	1.25	1.25	4.04	12
DPhPMPO/$O_2^{\bullet-}$	H_2O_2	pyridine	1.20	1.16	4.49	-
EDPhPN/$HO^{\bullet}$	H_2O_2-Fe^{2+}	PBS	1.41	0.19	2.92	
EDPhPN/$O_2^{\bullet-}$	HX-XO	PBS	1.34	0.19	2.92	
PDPhPN/$HO^{\bullet}$	H_2O_2-Fe^{2+}	PBS	1.70	0.45	4.71	
PDPhPN/$O_2^{\bullet-}$	HX-XO	PBS	1.36	-	3.18	
PDPhPN/$O_2^{\bullet-}$	H_2O_2	pyridine	1.30	-	3.38	

In the spin trapping experiment of Bu^{t}S$^\bullet$ and, GS$^\bullet$ generated from photo-cleavage of corresponding disulfide in phosphate buffer, the signal of these radical adducts were observed by using DPhPMPO (Figure 4). The hfsc's were calculated by the computer simulation of the experimental spectra. The calculated values were similar to the corresponding values of carbon and oxygen centered radical adducts and not much difference was observed.

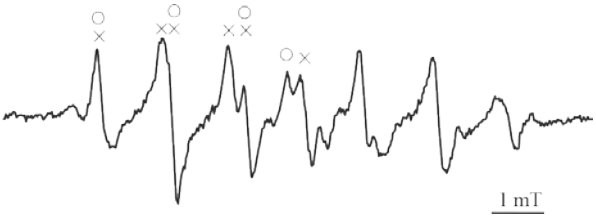

Figure 3 Spin trapping of LO$^\bullet$ with DPhPMPO. (○) indicates the signal of HO$^\bullet$ adduct and (×) indicates LO$^\bullet$ adduct.

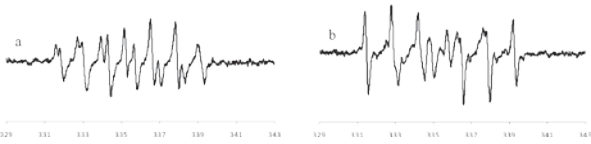

Figure 4 Spin Trapping of (a) *t*-BuS$^\bullet$ and (b) GS$^\bullet$ with DPhPMPO.

TABLE 2 ESR Hyperfine Splitting Constants for Spin Adduct of DPhPMPO

adduct	source	solvent	a_N (mT)	$a_{H\beta}$ (mT)	$a_{H\gamma}$ (mT)	a_P (mT)	conformer ratio / %
DPhPMPO/$CH_3^\bullet$	$CH_3I/(Bu_3Sn)_2$, $h\upsilon$	DMSO	1.05	1.41	0.04	3.83	86
			1.05	1.45	0.04	4.32	14
DPhPMPO/*t*-BuO$^\bullet$	*t*-BuOO-*t*-Bu, $h\upsilon$	DMSO	1.23	1.22	0.18	3.89	85
			1.23	1.22	0.18	4.32	15
DPhPMPO/ *t*-BuOO$^\bullet$	*t*-BuOOH, $h\upsilon$	DMSO	1.08	1.36	0.10	3.82	87
			1.08	1.36	0.10	4.32	13
DPhPMPO/$CH_3S^\bullet$	CH_3SSCH_3, $h\upsilon$	DMSO	1.26	1.25	0.04	3.96	95
			1.26	1.25	0.04	4.38	5
DPhPMPO/ *t*-BuS$^\bullet$	*t*-BuSS-*t*-Bu, $h\upsilon$	DMSO	1.26	1.26		3.48	50
			1.20	1.20		4.05	50
DPhPMPO/GS$^\bullet$	GSSG, $h\upsilon$	PBS	1.44	1.45		3.73	

(c) Spin Trapping of Other Radicals with Linear Spin Traps. Spin trapping experiments using linear spin traps substituted on alkyl moiety of PBN were described in the literature [28, 29]. However, for my knowledge, there is no report for substituent effect on carbon atom of C=N. Therefore, spin trapping experiments of carbon, oxygen and sulfur centered radicals with EDPhPN or PDPhPN were carried out (Scheme 3). Each signal of several radical adducts was observed as single conformation. These hfsc's were shown in Table 3. It was difficult to distinguish radical species adding to linear spin traps because the difference of hfsc's toward nitrogen atom of radical adduct were smaller than that of DPhPMPO. However, the a_P values for thiyl radical adduct of EDPhPN and PDPhPN were smaller than that of carbon and oxygen centered radical adducts. The tendency appeared in GS$^\bullet$ trapping experiment. The signal intensities of PDPhPN/R$^\bullet$ were slightly weaker than that of EDPhPN/R$^\bullet$. These differences increased proportional to the steric hindrance of alkyl moiety (Figure 4).

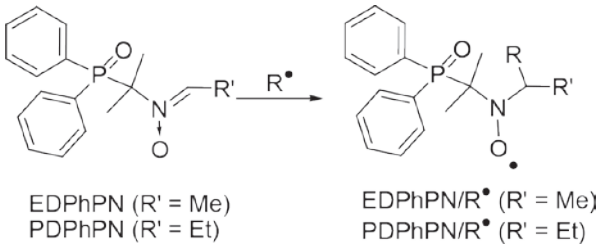

Scheme 3 Spin Trapping of Several Radicals with Linear Spin Traps

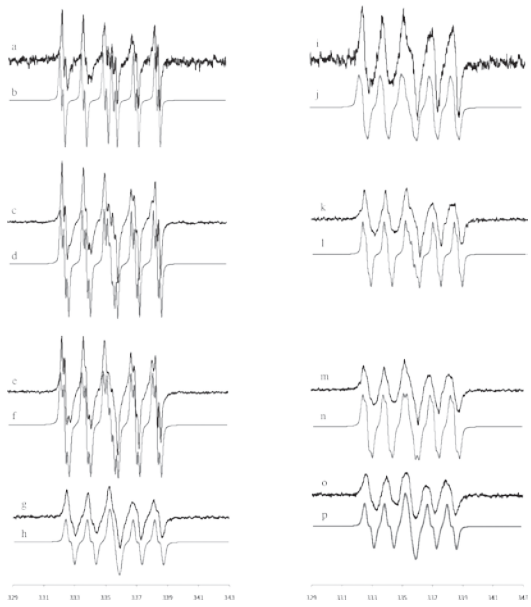

Figure 5 ESR Signals of Several Radical Adducts of EDPhPN and PDPhPN and Their Computer Simulation. (a) EDPhPN/$^{\bullet}CH_3$. (b) Computer simulation of (a). (c) EDPhPN/*t*-BuO$^{\bullet}$. (d) Computer simulation of (c). (e) EDPhPN/*t*-BuOO$^{\bullet}$. (f) Computer simulation of (e). (g) EDPhPN/$CH_3S^{\bullet}$. (h) Computer simulation of (g). (i) PDPhPN/$^{\bullet}CH_3$. (j) Computer simulation of (i). (k) PDPhPN/*t*-BuO$^{\bullet}$. (l) Computer simulation of (k). (l) PDPhPN/*t*-BuOO$^{\bullet}$. (m) Computer simulation of (l). (n) PDPhPN/$CH_3S^{\bullet}$. (o) Computer simulation of (n)

(d) Spin Trapping of Bulky S-centered Radicals with Linear Spin Traps

Spin trapping experiments of bulky S-centered radicals such as *t*-BuS$^{\bullet}$ and GS$^{\bullet}$ with linear spin traps were carried out under the similar conditions of DPhPMPO (Scheme 4). The ESR signal of the Bu^{t}S$^{\bullet}$ and GS$^{\bullet}$ adducts of PDPhPN was much weaker than that of corresponding EDPhPN adducts (Figure 6). The reaction rate of DMPO with GS$^{\bullet}$ was 1.6 times faster than that of PBN [30]. The signal/noise ratio of ESR spectra indicates that the signal intensity of DPhPMPO/ *t*-BuS$^{\bullet}$ or GS$^{\bullet}$ was stronger than that of linear spin trap under the same reaction conditions (Figure 4 and 6). The result implies that the addition of bulky S-centered radicals for DPhPMPO was faster than that of linear spin traps. On the other hand, a substituent effect of adjacent to imino double bond (C=N) was not well known. Significant difference for the trapping ability of linear spin traps toward bulky radical suggests that the reactivity of PDPhPN toward sterically congested radicals was lower than that of EDPhPN because of the steric hindrance around the C=N bond in PDPhPN. The reactivity of linear spin traps was affected by small sterically change such as one carbon number of alkyl chain.

TABLE 3 ESR Hyperfine Splitting Constants for Spin Adducts of EDPhPN and PDPhPN

adduct	source	a_N (mT)	a_H (mT)	a_H (mT)	a_P (mT)
EDPhPN/$CH_3^{\bullet}$	$CH_3I/(Bu_3Sn)_2$, $h\upsilon$	1.35	0.19	0.04	3.13
EDPhPN /*t*-BuO$^{\bullet}$	*t*-BuOO-*t*-Bu, $h\upsilon$	1.36	0.23	0.15	3.06
EDPhPN /*t*-BuOO$^{\bullet}$	*t*-BuOOH, $h\upsilon$	1.33	0.23	0.17	3.03
EDPhPN /$CH_3S^{\bullet}$	CH_3SSCH_3, $h\upsilon$	1.35	0.29	0.11	2.88
PDPhPN/$CH_3^{\bullet}$	$CH_3I/(Bu_3Sn)_2$, $h\upsilon$	1.35	0.24	0.19	3.13
PDPhPN /*t*-BuO$^{\bullet}$	*t*-BuOO-*t*-Bu, $h\upsilon$	1.35	0.23	0.15	3.08
PDPhPN /*t*-BuOO$^{\bullet}$	*t*-BuOOH, $h\upsilon$	1.31	0.25	0.20	3.02
PDPhPN /$CH_3S^{\bullet}$	CH_3SSCH_3, $h\upsilon$	1.29	0.32	0.11	2.78

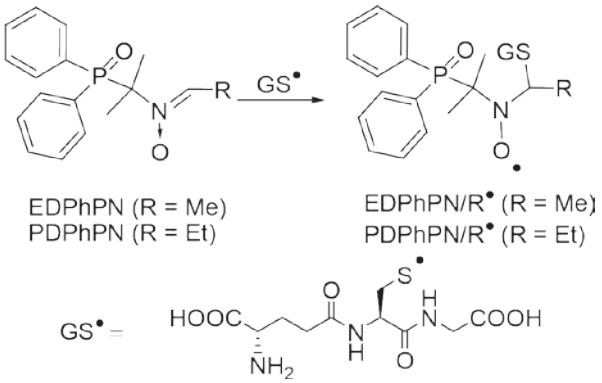

Scheme 4 Spin Trapping of GS$^{\bullet}$ with EDPhPN or PDPHPN.

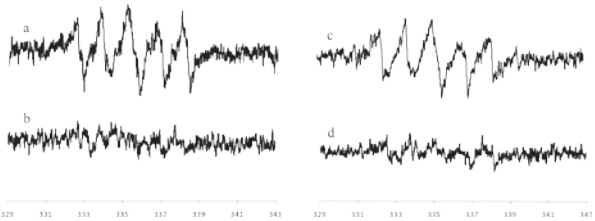

Figure 6 ESR Spectra of (a) EDPhPN/Bu^{t}S$^{\bullet}$, (b) PDPhPN/Bu^{t}S$^{\bullet}$, (c) EDPhPN/GS$^{\bullet}$ and (d) PDPhPN/GS$^{\bullet}$.

Summary

The study showed that the cyclic and linear spin traps containing diphenylphosphinoyl moiety successfully detected hydroxyl and superoxide anion radical as well as alkyl, alkoxy, peroxy, and thiyl radical. The trapping ability of the linear traps was influenced by the steric factor of alkyl chain of a spin trap and radical species. The difference in the reactivity between cyclic and linear spin traps might be a useful tool to distinguish radical species generated *in vivo.*

Acknowledgements

We thank Mr. Taisuke Matsumoto (Analytical Center, Institute for Materials Chemistry and Engineering, Kyushu University) for X-ray crystalographic analysis for structure of EDPhPN and PDPhPN

Experimentals

Materials. The solvents were distilled under nitrogen atmosphere. All chemicals were obtained from commercial supplier and used without further purification. DPhPMPO was synthesized according to the literature. Ghost erythrocyte cell was prepared by the methods previously reported in the literature. Analytical TLC was carried out on precoated plates (Merck, silica gel 60, F254) and flush column chromatography was performed with silica (Merck, 70-230 mesh). NMR spectra (^{1}H at 400 MHz; ^{13}C at 100 MHz; ^{31}P at 161MHz) were recorded in $CDCl_3$ solvent, and the chemical shifts were expressed in ppm relative to internal TMS. ^{31}P NMR was taken in $CDCl_3$ using 85% H_3PO_4 as an internal standard with broadband ^{1}H decoupling. ESR spectra were recorded at room temperature using a spectrometer at 9.5 GHz employing 100 kHz field modulation. The melting points were uncorrected.

General Procedure for Synthesis of Linear Spin Traps. Ethylamine or propylamine (90 mmol) was mixed with 6.0 ml of acetone and 7.5 g of silica gel. After microwave irradiation for 1 min, the reaction mixture was dissolved in CH_2Cl_2 and filtrated. The filtrate was concentrated *in vacuo*. The residue was mixed with 8.5 mmol of diphenylphosphine oxide **1** and 4.3 g of silica gel. The reaction mixture was irradiated with microwave for 1 min. The reaction mixture was dissolved in CH_2Cl_2 and filtrated. The filtrate was concentrated to give a crude mixture of propylidene amine **2**. The purification was carried out by recrystallization to give amine **2** as colorless crystals. The solution of amine **2** (3.2 mmol) in 15 ml of acetone was added 16 mL of aq. $NaHCO_3$ (1.1g, 13 mmol) and 50 mL of aq. Oxone (2.4g, 3.8 mmol) dropwise at 0°C. After stirring for 10 h at room temperature, the reaction mixture was quenched by 16 mL of 10% sodium thiosulfate and acetone was removed under reduced pressure. The residue was extracted with CH_2Cl_2 (50 mL x 3) and dried over $MgSO_4$. The organic layer was concentrated to give a pale yellow oil, which was recrystallized from water-acetonitrile to give nitrone.

Ethylidene-1-diphenylphosphoryl-1-methylethylamine *N*-oxide (EDPhPN); colorless crystals. mp 119.0-119.5 °C. ^{1}H NMR ($CDCl_3$) δ 1.75 (6H, d, J = 12.01), 1.86-1.85 (3H, m), 6.90-6.85 (1H, m), 7.54-7.44 (6H, m) 8.18-8.13 (4H, m); ^{13}C NMR ($CDCl_3$) δ 13.25, 23.02, 74.04, 74.79, 128.32, 128.44, 129.28, 130.26, 132.20, 132.23, 132.98, 133.07, 133.55, 133.59; ^{31}P NMR ($CDCl_3$) δ 37.6; Anal. Calcd for $C_{17}H_{20}NO_2P$: C, 67.76; H, 6.69; N, 4.65. Found: C, 67.71; H, 6.67; N, 4.62.

Propylidene-1-diphenylphosphoryl-1-methylethylamine *N*-oxide (PDPhPN); colorless crystals. Mp 91-92°C. ^{1}H NMR ($CDCl_3$) δ = 0.91(t, 3H, J= 7.6 Hz), 1.75 (d, 6H, $J_{P\text{-}H}$ = 12.8 Hz), 2.30 (m, 2H), 6.69 (m, 1H), 7.44-7.54 (6H, m), 8.141-8.189 (4H, m). ^{13}C NMR ($CDCl_3$) δ = 10.0, 20.1, 23.1, 74.3 ($J_{P\text{-}C}$ = 75.6 Hz), 128.3, 128.4, 129.3, 130.3, 132.2, 133.0, 133.1 139.5($J_{P\text{-}C}$ = 5.0 Hz). ^{31}P NMR ($CDCl_3$) δ = 37.9. Anal. Calcd for $C_{18}H_{22}NO_2P$: C, 68.56; H, 7.03; N, 4.44. Found: C; 68.93; H, 7.11; N, 4.42.

Spin Trapping Studies. (a) ESR Measurement. ESR spectra were recorded at room temperature using a spectrometer at 9.5 GHz employing 100 kHz field modulation. Reaction mixture was prepared in a phosphate buffer (1.0 M, pH 7.4).

(b) Hydroxyl Radical Adduct: Fenton reaction system. A standard Fenton reaction system was employed to generate $HO^{\bullet}$. $FeCl_3$ was added to a solution containing 0.1 M phosphate buffer, 0.1 M spin traps, 10 mM of H_2O_2.

(c) Superoxide Adduct: Hypoxanthine-Xanthine Oxidase System. This superoxide generating system contained 0.4 mM of hypoxanthine, 0.5 unit ml^{-1} xanthine oxidase and 0.1 M of spin traps in 0.1 M phosphate buffer. Oxygen was bubbled into the reaction mixture for 30 s and then the ESR spectrum was recorded 40 s after the addition of xanthine oxidase. **H_2O_2/Pyridine System.** H_2O_2 was added to a deoxygenated solution of PDPHPN or DPhPMPO in pyridine.

(d) *tert*-Butylperoxyl Radical Trapping: *t*-BuOOH/*hυ* system. The *tert*-butylperoxyl radical adduct was generated by photolysis of *t*-BuOOH (1.5 M) in the presence of a spin trap in deoxygenated benzene.

(e) *tert*-Butoxyl Radical Trapping: *t*-BuOO-*t*-Bu/*hυ* system. The *tert*-butoxyl radical radical adduct was generated by photolysis of *t*-BuOO-*t*-Bu (0.5 M) in the presence of a spin trap in deoxygenated benzene.

(f) Methyl Thiyl Trapping. Methylthiyl radical adduct was generated by photolysis of EtSSEt (1.0 M) in the presence of a spin trap in deoxygenated benzene.

(g) Methyl Radical Trapping. A Fenton reaction system in the presence of DMSO was used to generate $^{\bullet}CH_3$ and added to a phosphate buffer solution containing a spin trap (10 mM), H_2O_2 (1.0 mM), and DMSO (10%).

(h) GS$^{\bullet}$ Radicals Trapping: GSSG/*hυ* system. A 50-μL aliquot of 0.1 M phosphate buffer solution containing 30 mM spin traps and 100 mM GSSG was prepared. The radical was generated by UV photolysis. The EPR spectra of adducts were recorded over a 5 min period.

(i) Linoleyl Peroxyl Adduct: LOOH/Toluene System. 13-(*S*)-hydroperoxy-9*Z*,11*E*-octadecadienoic acid (1.5 M) was added to a deoxygenated solution spin traps (20 mM) in toluene and photolyzed for 30 s.

Crystal structure of linear spin traps EDPhPN and PDPhPN

The crystal structures of EDPhPN and PDPhPN were determined using a Rigaku Saturn CCD area detector with graphite-monochromated Mo-Kα radiation and a rotating anode generator. The unit-cell parameters were determined by the least-square refinement of 25 reflections. The intensity data were collected at room temperature by the ω-2θ technique up to a maximum 2θ value of 60.0°. The structure was solved according to the heavy-atom Patterson method, and expanded using Fourier techniques. The non-hydrogen atoms were refined anisotropically, while the hydrogen atoms were refined isotropically. The final cycle of the full-matrix least-squares refinement was based on 28910 (EDPhPN) and 28939 (PDPhPN), observed reflections ($I > 2.00\ \sigma\ (I)$) and 398 for EDPhPN and 404 for PDPhPN variable parameters, and converged with the unweighted and weighted agreement factors of R (R_W) = 0.0949 (0.2251) for EDPhPN and 0.0800 (0.1674) for PDPhPN. All calculations were determined using the SHELXL crystallographic package.

References

1 Singh KK, editors. Oxidative stress, Disease and Cancer. London: Imperial College Press; 2006. And references therein.

2 Janzen EG, Poyer JL, Schaefer CF, Downs PE, Dubose CM. Biological spin trapping II. Toxicity of nitrone spin traps: dose-ranging in the rat. J. Biochem. Biophys. Methods 1995; 30: 239-247.

3 Finkelstein E, Rosen GM, Rauckman EJ. Spin trapping of superoxide and hydroxyl radical: Practical aspects. Arch. Biochem. Biophys. 1980; 200; 1-16.

4 Janzen EG. Free Radicals in Biology. Pryor WA, editors. New York: Academic Press; 1980. Vol. 4, p 115-154.

5 Harbour JR, Chow V, Bolton JR. An electron spin resonance study of the spin adducts of OH and HO_2 radicals with nitrones in the ultraviolet photolysis of aqueous hydrogen peroxide solutions Can. J. Chem. 1974; 52: 3549-3553.

6 Frejaville C, Karoui H, Tuccio B, Moigne FL, Culcasi M, Pietri S, Lauricella R, Tordo P. 5-(Diethoxyphosphoryl)-5-methyl-1-pyrroline N-oxide: A new efficient phosphorylated nitrone for the *in vitro* and *in vivo* spin trapping of oxygen-centered radicals. J. Med. Chem. 1995; 38: 258-265.

7 Roubaud V, Sankarapandi S, Kuppusamy P, Tordo P, Zweier JL. Quantitative measurement of superoxide generation and oxygen consumption from leukocytes using electron paramagnetic resonance spectroscopy. Anal. Biochem. 1998; 257: 210-217.

8 Roubaud V, Sankarapandi S, Kuppusamy P, Tordo P. Zweier JL. Quantitative measurement of superoxide generation using the spin trap 5-(Diethoxyphosphoryl)-5-methyl-1-pyrroline-*N*-oxide. Anal. Biochem. 1997; 247: 404-411.

9 Nolth JA, Spector AA, Buettner GR. Detection of lipid radicals by electron paramagnetic resonance spin trapping using intact cells enriched with polyunsaturated fatty acid. J. Biol. Chem. 1992; 267: 5743-5746.

10 Zeghdaoui A, Tuccio B, Finet J-P, Cerri V, Tordo P. β-Phosphorylated α-phenyl-*N*-*tert*-butylnitrone (PBN) analogues: a new series of spin traps for oxyl radicals. J. Chem. Soc., Perkin Trans. 2 1995; 2087-2089.

11 Liu Y-P, Wang L-F, Nie Z, Ji Y.-Q, Liu Y, Liu K-J, Tian Q. Effect of the phosphoryl substituent in the linear nitrone on the spin trapping of superoxide radical and the stability of the superoxide adduct: combined experimental and theoretical studies. J. Org. Chem. 2006; 71: 7753-7762.

12 Nishizawa M, Shioji K, Kurauchi Y, Okuma K, Kohno M. Spin-trapping properties of 5-(diphenylphosphinoyl)-5-methyl-4,5-dihydro-3H-pyrrole N-oxide (DPPMDPO). Bull. Chem. Soc. of Jpn. 2007; 80: 495-497.

13 Shioji K, Matsumoto A, Takao M, Kurauchi Y, Shigetomi T, Yokomori Y, Okuma K. Cycloadditions of 3,4-dihydro-2H-pyrrole *N*-oxide with thioketones and a selenoketone. Bull. Chem. Soc. of Jpn. 2007; 80: 743-746.

14 Shioji K, Tsukimoto S, Tanaka H, Okuma K. Synthesis of 5-(alkylphenylphosphoryl)-5-methyl-3, 4-dihydro-2H-pyrroline N-oxide as a new spin trapping reagent. Chem. Lett. 2003; 32: 604-605.

15 Shioji K, Takao M, Okuma K. Convenient synthesis of linear spin traps containing diphenylphosphoryl groups. Chem. Lett. 2006; 1332-1333.

16 Shioji K, Iwashita H, Shimomura T, Yamaguchi T, Okuma K. ESR measurement using 2-diphenylphosphinoyl-2-methyl-3,4-dihydro-2H-pyrrole *N*-oxide (DPhPMPO) in human erythrocyte ghosts. Bull. Chem. Soc. of Jpn. 2007; 80: 758-762.

17 Sawa T, Akaike T, Kida K, Fukushima Y, Takagi K, Maeda H. Lipid peroxyl radicals from oxidized oils and heme-iron: implication of a high-fat diet in colon carcinogenesis. Cancer Epidemiol. Biomarkers Prev. 1998; 7: 1007-1012.

18 Dikalov SI, Mason RP. Spin trapping of polyunsaturated fatty acid-derived peroxyl radicals: reassignment to alkoxyl radical adducts. Free Radic. Biol. Med. 2001; 30: 187-197.

19 Qian SY, Wang HP, Schafer FQ, Buettner GR. EPR detection of lipid-derived free radicals from PUFA, LDL, and cell oxidations. Free Radic. Biol. Med. 2000; 29: 568-579.

20 Schafer FQ, Buettner GR. Redox state of the cell as viewed though the glutathione disulfide/glutathione couple. Free Radic Biol Med. 2001; 30: 1191-1212.

21 Kalyanaraman B, Karoui H, Singh RJ, Felix CC. Detection of thiyl radical adducts formed during hydroxyl radical- and peroxynitrite-mediated oxidation of thiols—a high resolution ESR spin-trapping study at Q-band (35 GHz). Anal. Biochem. 1996; 241: 75-81.

22 Karoui H, Hogg N, Joseph J, Kalyanaraman B. Effect of superoxide dismutase mimics on radical adduct formation during the reaction between peroxynitrite and thiols—an ESR-spin trapping study. Arch. Biochem. Biophys. 1996; 330: 115-124.

23 Augusto O, Gatti RM, Radi R. Spin-trapping studies of peroxynitrite decomposition and of 3-morpholinsydnonimine N-ethylcarbamide autooxidation: direct evidence for metal-independent formation of free radical intermediates. Arch. Biochem. Biophys. 1994; **310**: 118-125.

24 Xu YK, Chen ZW, Sun J, Liu K, Chen W, Shi W, Wang HM, Liu Y. Synthesis, crystal structure, and ESR study of a novel phosphorylated lipophilic spin trap. J. Org. Chem. 2002; 67: 7624-7630.

25 O'Brien PJ. Intracellular mechanisms for the decomposition of a lipid peroxide. I. Decomposition of a lipid peroxide by metal ions, heme compounds, and nucleophiles. Can. J. Biochem. 1969; 47: 485-492.

26 Stolze K, Udilova N, Nohl H. Lipid radicals: Properties and detection by spin trapping. Acta. Biochim. Polon, 2000; 47: 923-930.

27 Bartsch H, Nair J, Owen RW. Dietary polyunsaturated fatty acids and cancers of the breast and colorectum: emerging evidence for their role as risk modifiers. Carcinogenesis, 1999; 20: 2209-2218.

28 Gamliel A, Afri M, Frimer AA. Determining radical penetration of lipid bilayers with new lipophilic spin traps. Free Radic. Biol. Med. 2008; 44: 1394-1405.

29 Stolze K, Udilova N, Rosenau T, Hofinger A, Nohl H. Spin trapping of superoxide, alkyl- and lipid-derived radicals with derivatives of the spin trap EPPN. Biochem. Pharmacol. 2003; 66: 1717-1726.

30 Polovyanenko DN, Plyusnin VF, Reznikov VA, Khramtsov VV, Bagryanskaya EG. Mechanistic studies of the reactions of nitrone spin trap PBN with glutathiyl radical. J. Phys. Chem. B. 2008; 112: 4841-4847.